Journal of Experimental and Theoretical Physics, Vol. 97, No. 5, 2003, pp. 969–977.
Translated from Zhurnal Éksperimental'noĭ i Teoreticheskoĭ Fiziki, Vol. 124, No. 5, 2003, pp. 1080–1089.

SOLIDS
Structure

Nonadiabatic Interaction of Acoustic Phonons with Spins $S = 1/2$ in the Two-Dimensional Heisenberg Model

S. S. Aplesnin

Kirenskiĭ Institute of Physics, Siberian Division, Russian Academy of Sciences, Akademgorodok, Krasnoyarsk, 660036 Russia

e-mail: apl@iph.krasn.ru

Received February 27, 2003

Abstract—The ground state of a two-dimensional antiferromagnet having spins $S = 1/2$ and interacting with acoustic phonons is investigated in the nonadiabatic approximation using the quantum-mechanical Monte Carlo method. The critical parameters of the spin–phonon coupling, corresponding to the formation of bound spin–phonon excitations, crystal symmetry lowering, and the emergence of a gap in the spin excitation spectrum, as well as the antiferromagnet–quantum spin liquid transition, are determined. The orthorhombicity parameter, the sublattice magnetization, the violation of the spherical symmetry of spin–spin correlation functions, and the magnetic moment in Gd_2CuO_4 and Eu_2CuO_4 are calculated. © *2003 MAIK "Nauka/Interperiodica".*

1. INTRODUCTION

Intense studies of electronic, elastic, and magnetic properties of high-temperature superconductors and manganites with a colossal magnetoresistance have lead to the conclusion that the electronic structure is closely related to magnetic and lattice fluctuations. For weakly doped superconducting cuprates, one of the hypotheses is associated with the formation of a quasigap due to the generation of coupled spin–phonon excitations. This hypothesis is confirmed by the results of optical measurements [1]; for example, Raman spectra are explained on the basis of coupled excitations in a system consisting of two magnons and a phonon. In the low-temperature range, a number of observed structural distortions are due to lattice modulation, and superstructural reflections exhibit tetragonal symmetry as well as symmetry lower than the orthorhombic symmetry. For $La_{1.6-x}Nd_{0.4}Sr_xCuO_4$, these transitions exist in the normal phase at $T < 80$ K [2]. In $La_{2-x}Sr_xCuO_4$ ($x < 0.05$), the isotopic effect is observed with an intensity comparable to that for traditional superconductors [3]. Another feature of weakly doped semiconducting cuprates is associated with their thermal conductivity, which cannot be described using the theory of a Fermi liquid and presumes the existence of certain delocalized quasiparticles [4]. These experimental facts indicate the existence of two characteristic energy scales: the electron–phonon and the spin–phonon interactions.

Some peculiarities in magnetic properties, which are also observed in allied compounds with a tetragonal T' structure and with CuO planes in R_2CuO_4 (R = Eu, Gd, Nd), can be due to the interaction between lattice and spin fluctuations. Such compounds are characterized by low values of the magnetic moment of copper ions ($\sigma \approx 0.4$) and a relatively high Néel temperature ($T_N \approx 230$–280 K). The following has been observed: strong anharmonicity in local displacements in the CuO plane in the temperature range $145 \text{ K} < T < 175$ K in the absence of structural transitions up to 393 K and a minimum in the temperature dependence of the square of average displacements of copper ions along the [100] direction at $T = 175$ K [5] due to antiferromagnetic spin fluctuations. The antiferromagnet Gd_2CuO_4 with a tetragonal symmetry exhibits the electron spin resonance at $\omega_0 = 18.2$ cm^{-1} [6], which can be explained by the orthorhombic distortion of lattice planes with a stochastic arrangement of the orthorhombicity vectors along the c axis. At $T = 20$ K, the resonance disappears and the susceptibility increases strongly [7], which can be attributed to the coherent orthorhombicity state (although the elastic scattering of neutrons and X-ray studies do not confirm this effect). These effects are probably associated with the formation of bound spin–phonon quasiparticles, i.e., lattice and spin fluctuations coupled dynamically with each other.

Antiferromagnets with the spin–phonon interaction were considered in the adiabatic approximation, in which the interaction between spin and acoustic phonons can be reduced to the four-spin exchange interaction and to the effective interaction between the spins of next-to-nearest neighbors. For certain parameters of this model, a spin nematic state with violation of the spherical symmetry of the spin–spin correlation functions is formed [8] and the long-range magnetic order disappears [9]. The interaction between the spin and the elastic subsystems leads to nonlinear interactions not only between spins, but also between phonons. For this reason, a correct solution should be carried out taking into account the nonadiabatic inter-

action between spins and phonons; this can be done using the quantum-mechanical Monte Carlo method based on the continuous-time algorithm.

2. COMPUTATIONAL MODEL AND METHOD

For quasi-two-dimensional magnets, the interplanar exchange is several orders of magnitude weaker than the intraplanar exchange; consequently, we can confine our analysis to the interaction between the spins of the nearest neighbors and with acoustic modes of vibrations in the plane of the lattice. In the harmonic approximation, the Hamiltonian for a coupled spin–phonon system has the form

$$\begin{aligned} H &= \sum_{i,j}[J+\alpha(u_{i,j}-u_{i+1,j})] \\ &\times\left[S^z_{i,j}S^z_{i+1,j}+\frac{1}{2}(S^+_{i,j}S^-_{i+1,j}+S^-_{i,j}S^+_{i+1,j})\right] \\ &+[J+\alpha(u_{i,j}-u_{i,j+1})] \\ &\times\left[S^z_{i,j}S^z_{i,j+1}+\frac{1}{2}(S^+_{i,j}S^-_{i,j+1}+S^-_{i,j}S^+_{i,j+1})\right] \\ &+\frac{1}{2}M\dot{u}^2_{i,j}+\frac{1}{2}K(u_{i,j}-u_{i+1,j})^2+\frac{1}{2}K(u_{i,j}-u_{i,j+1})^2, \end{aligned} \tag{1}$$

where $S^{z,\pm}$ are the components of the spin operator $S = 1/2$ at a lattice site, $u_{i,j}$ is the displacement of an ion over the translation vectors of the lattice, M is the ion mass, and K is the elastic rigidity constant of the lattice ($J > 0$). Using the canonical transformation

$$\hat{u}_{\mathbf{r}} = \frac{1}{\sqrt{N}}\sum_{\mathbf{q}}\sqrt{\frac{\hbar}{2M\Omega(\mathbf{q})}}(b_{\mathbf{q}}+b^+_{-\mathbf{q}})e^{i\mathbf{q}\cdot\mathbf{r}}, \tag{2}$$

we pass from variables $u_{i,j}$ to the creation ($b^\dagger$) and annihilation (b) operators of phonon with momenta $q_\beta = 2\pi n/L$, $n = 1, 2, \ldots, L$, where $\beta = x, y$ and the lattice constant $a = 1$. The transformed Hamiltonian has the form

$$\begin{aligned} H &= \sum_{i,j}J_{i,j}\mathbf{S}_i\cdot\mathbf{S}_j+\sum_{q_x,q_y}\sum_{n,m}\alpha\sqrt{\frac{\hbar}{2M\Omega(\mathbf{q})}}e^{i\mathbf{q}\cdot\mathbf{r}} \\ &\times(b_{\mathbf{q}}+b^+_{-\mathbf{q}})[(1-\cos q_x-i\sin q_x)\mathbf{S}_{n,m}\cdot\mathbf{S}_{n+1,m} \\ &+(1-\cos q_y-i\sin q_y)\mathbf{S}_{n,m}\cdot\mathbf{S}_{n,m+1}] \\ &+\sum_{\mathbf{q}}\hbar\Omega(\mathbf{q})b^\dagger_{\mathbf{q}}b_{\mathbf{q}}, \end{aligned} \tag{3}$$

where $\Omega(\mathbf{q}) = \omega_0\sqrt{2-\cos q_x-\cos q_y}$ and $\omega_0 = \sqrt{2K/M}$.

In computations, the spin–phonon interaction constant α and the excitation energy ω normalized to exchange are used. As the computational method, we choose the quantum-mechanical Monte Carlo method combining the algorithms of world lines and continuous time [10] on a plane of dimensions $N = 32\times 32$ with periodic boundary conditions at temperature $\beta = J/T = 50$. In accordance with this method, the Hamiltonian is divided into three parts: the diagonal part,

$$H_0 \propto JS^z_iS^z_j+\hbar\Omega(\mathbf{q})n_{\mathbf{q}},$$

where $n_{\mathbf{q}}$ is the occupation number of phonons with the same momentum; and two nondiagonal parts,

$$V_J \propto \frac{J}{2}(S^+_iS^-_j+S^-_iS^+_j),$$

$$V_\alpha \propto \alpha\sqrt{\frac{\hbar}{M\Omega(\mathbf{q})}}(b_{\mathbf{q}}+b^\dagger_{-\mathbf{q}})\hat{S}_i\hat{S}_j.$$

Applying the Trotter formula [11], we can disregard the commutation of operators V_j and V_α to within $\tau_0^2\alpha J/(2\sqrt{\omega_0})$. This leads to a systematic error whose maximal value is 15% for $\alpha = 4$, $\omega_0 = 8$, and $\tau_0 = 0.5$. Following [10] we express operators $\exp[-\tau_0(H_0/2 + V_J)]$ and $\exp[-\tau_0(H_0/2 + V_\alpha)]$ on the imaginary time segment τ_0 in terms of the evolution operator σ_{ev} in the interaction representation $\exp(-\tau_0 H) = \exp(-\tau_0 H_0)\sigma_{ev}$, where

$$\begin{aligned} \sigma_{ev} &= 1-\int_0^{\tau_0}d\tau V_{J,\alpha}(\tau)+\ldots+(-1)^m \\ &\times\int_0^{\tau_0}d\tau_m\ldots\int_0^{\tau_2}d\tau_1 V_{J,\alpha}(\tau_m)\ldots V_{J,\alpha}(\tau_1)+\ldots, \end{aligned} \tag{4}$$

and

$$V_{J,\alpha}(\tau) = e^{\tau H_0}V_{J,\alpha}e^{-\tau H_0}, \quad V_{J,\alpha}|\beta\rangle = -q_{\gamma\beta}(J,\alpha)|\gamma\rangle.$$

Summation and integration of two operators V_J and V_α in Eq. (4) are carried out using a stochastic procedure of sampling various kink–antikink configurations in accordance with their weights. The probability of the formation of a kink–antikink pair is given by

$$W = |q_{\gamma\beta}(J,\alpha)|^2\exp[(\tau_2-\tau_1)E_{\gamma\beta}], \quad \tau_2-\tau_1<\tau_0.$$

A subprocess of kink shift along the time axis with probability $W = \exp(\Delta\tau E_{\gamma\beta})$ is possible. The use of global spin flips at a site and a change in the occupation number of phonons with momentum q lead to a finite transition probability $W \sim q_{\gamma\beta}$ on interval τ_0. As a result,

the total projection of the spin changes and discontinuities are observed on world lines with even numbers. Since computations lead to only an even number of nondiagonal changes of trajectories $q_{\gamma\beta}^{2n}(J)$ and $q_{\gamma\beta}^{2n}(\alpha)$, we can avoid obtaining the minus sign due to an increase in the systematic error. As an eigenfunction of Hamiltonian H_0, we choose the S^z representation of $\uparrow$ and $\downarrow$ spins; the occupation numbers of phonons with momentum $\mathbf{q}$ are $n_\mathbf{q} = 0, 1, 2, \ldots$ (the maximum number is not limited).

The spectral density of magnetic and spin–phonon excitations can be determined from the corresponding time correlation functions calculated in imaginary time for $\tau > 0$. We define the spin correlator in the form

$$\begin{aligned}\langle S^-(\tau)S^+(0)\rangle \\ = \sum_\nu |\langle \nu|S^+|\mathrm{vac}\rangle|^2 \exp[-(E_\nu - E_0)\tau],\end{aligned} \tag{5}$$

where $|\nu\rangle$ is the complete set of eigenstates of Hamiltonian H_0, $H_0|\nu\rangle = E_\nu|\nu\rangle$, $H_0|\mathrm{vac}\rangle = E_0|\mathrm{vac}\rangle$. For the vacuum state, we choose the Néel arrangement of spins with energy $E_0/NJ = 1/4$. Let us redefine the spin correlator (5) as

$$\begin{aligned}\langle S^-(\tau)S^+(0)\rangle &= \int_0^\infty d\omega \rho_s(\omega) e^{-\omega\tau}, \\ \rho_s(\omega) &= \sum_\nu \delta(\omega - \Omega_\nu)|\langle \nu|S^+|\mathrm{vac}\rangle|^2, \\ \Omega_\nu &= E_\nu - E_0,\end{aligned} \tag{6}$$

where $\rho_s(\omega)$ defines the spectral density of magnetic excitations. We treat spin–phonon excitations as coupled excitations of spins, appearing as a result of action of operators $\hat{S}^z$ and $\hat{S}^+$, and phonons induced by the creation operators $b^\dagger$ on the wave function of vacuum $n_\mathbf{q} = 0$. We represent the time correlators in the form

$$\begin{aligned}\langle b(\tau)S^z(\tau)b^\dagger(0)S^z(0)\rangle &= \sum_\nu |\langle \nu|b^\dagger S^z|\mathrm{vac}\rangle|^2 \\ &\times \exp[-(E_\nu - E_0)\tau], \quad \tau \geq 0, \\ \langle b(\tau)S^-(\tau)b^\dagger(0)S^+(0)\rangle &= \sum_\gamma |\langle \nu|b^\dagger S^+|\mathrm{vac}\rangle|^2 \\ &\times \exp[-(E_\gamma - E_0)\tau], \quad \tau \geq 0.\end{aligned} \tag{7}$$

Analogously to (6), we define the spectral density of coupled spin–phonon excitations in the form

$$\rho_{sp}(\omega) = \rho_{bS^z}(\omega) + \rho_{bS^-}(\omega).$$

In fact, the Monte Carlo method is used for calculating the time correlator on a finite interval $0 < \tau < \tau_0$. In order to reproduce the spectral density in a wide range of energies, we must solve the integral equation (6). For this purpose, we use the stochastic procedure optimizing the deviation [12]

$$D = \int_0^{\tau_0} |G(\tau) - G_t(\tau)|G^{-1}(\tau)d\tau \tag{8}$$

of the computed correlator $G(\tau)$ from the true correlator $G_t(\tau)$ with the spectral density $\rho_t(\omega)$.

In order to calculate the nondiagonal operators, we use a symmetrized representation of the wave function in the imaginary time interval τ_0. For example, we seek the eigenvalue of operators $(b_\mathbf{q}^\dagger, b_\mathbf{q})$ for $\tau \longrightarrow 0$ on the basis of the functions

$$\begin{aligned}\nu(\tau_i) &= c_1|n_{\mathbf{q}1}, n_{\mathbf{q}2}, n_{\mathbf{q}3}, \ldots\rangle \\ &+ c_2|n_{\mathbf{q}1} + 1, n_{\mathbf{q}2}, n_{\mathbf{q}3}, \ldots\rangle \\ &+ c_3|n_{\mathbf{q}1}, n_{\mathbf{q}2} + 1, n_{\mathbf{q}3}, \ldots\rangle + \ldots\end{aligned}$$

The displacement of an ion at a site is defined as

$$\begin{aligned}\langle u(\mathbf{r})\rangle &= \sqrt{\frac{\hbar}{2MN}} \\ &\times \sum_\nu \langle \nu_j|(b_\mathbf{q} + b_{-\mathbf{q}}^\dagger)e^{i\mathbf{q}\cdot\mathbf{r}}\Omega^{-1/2}(\mathbf{q})|\nu_j\rangle.\end{aligned} \tag{9}$$

The mean square displacement of the ion is defined as

$$\langle u^2\rangle = \frac{\hbar}{2MN}\sum_\mathbf{q} \frac{2n_\mathbf{q} + 1}{\Omega(\mathbf{q})}.$$

In the ground state, the number of phonons for a harmonic oscillator with $\alpha \longrightarrow 0$ is equal to zero. Therefore, it is important to calculate the change in zero-point vibrations as a result of action of the magnetic system on the elastic one; i.e.,

$$\langle U_n^2\rangle = \langle u^2(\alpha)\rangle - \langle u^2(\alpha = 0)\rangle.$$

In the subsequent analysis, we will use the quantities

$$\langle U\rangle = \frac{1}{N}\sum_r \frac{\langle u(r)\rangle}{\sqrt{\hbar/2MN\omega_0}}, \quad \langle U^2\rangle = \sum_r \frac{\langle U_n^2(r)\rangle}{\hbar/2NM\omega_0}.$$

Correlated vibrations of ions and their momentum dependence can be determined from the correlation

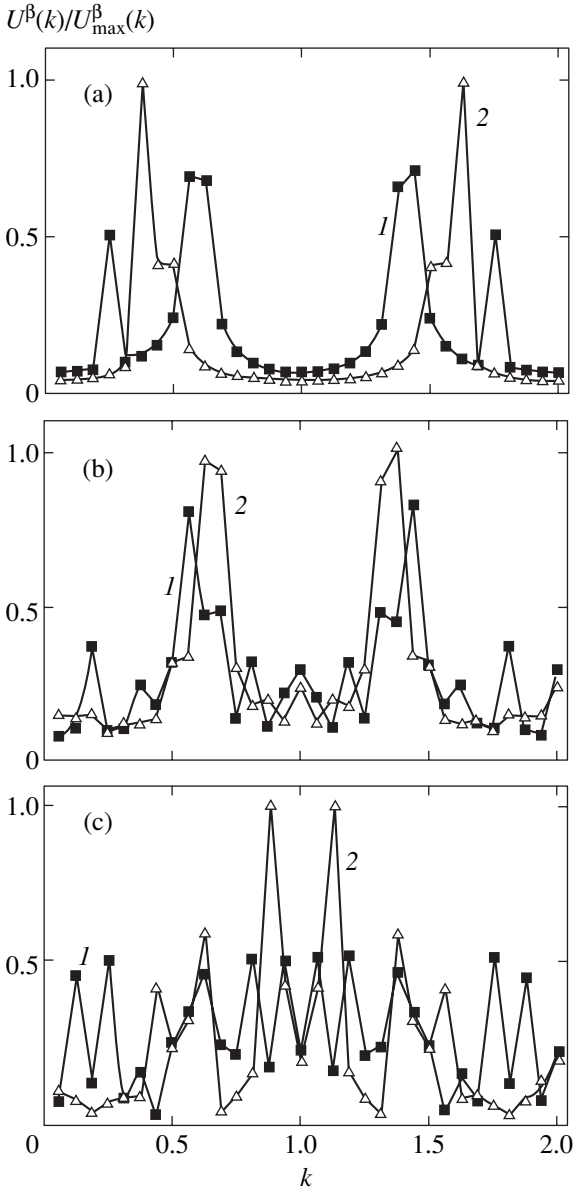

Fig. 1. The lattice structural factor $U^\beta(k)/U^\beta_{\max}(k)$ normalized to the maximum value and calculated in two directions β = [10] (*1*) and [01] (*2*) for $\omega_0/J = 6$, $\alpha/\alpha_{c3} = 0.3$ (a), 0.7 (b), and 1 (c).

phonon density function $\langle n(\mathbf{q})n(\mathbf{q}+\mathbf{p})\rangle$. The wave vectors of incommensurability of lattice and magnetic fluctuations were determined from the ion displacement structural factor

$$U(\mathbf{q}) = \frac{1}{N}\sum_{\mathbf{q}}\langle u_0 u_{\mathbf{r}}\rangle e^{i\mathbf{q}\cdot\mathbf{r}}$$

in two directions, [10] and [01], and the magnetic structural factor

$$S^z(\mathbf{k}) = \frac{1}{N}\sum_{\mathbf{k}}\langle S^z_0 S^z_{\mathbf{r}}\rangle e^{i\mathbf{k}\cdot\mathbf{r}}.$$

In the computational procedure, the first 20000 Monte Carlo steps per spin were omitted and the averaging was carried out over 8000 Monte Carlo steps per spin. This value is much larger than the time of attainment of thermodynamic equilibrium calculated from the sublattice magnetization,

$$\langle\sigma(0)\sigma(t)\rangle - \langle\sigma(0)\rangle\langle\sigma(\tau_{\max})\rangle = A\exp(-t/t_0),$$

where t is the number of Monte Carlo steps; t_0 = 3000 and 7000 Monte Carlo steps per spin for $\alpha/\alpha_c = 0.3$ and 0.75, respectively; and α_c is the critical parameter of the spin–phonon coupling, for which the long-range magnetic order disappears. The mean square error amounts approximately to 3% for the sublattice magnetization, 1% for the energy, 2% for the spin–spin correlation functions, and 4% for the average phonon occupation number.

3. DISCUSSION

The processes of inelastic scattering and formation of magnon and phonon bound states are determined by the density of states of the initial quasiparticles. In the two-dimensional Heisenberg model, the density of magnon states diverges logarithmically at the middle of the band and the interaction between quasiparticles is symmetric for points Γ and X of the band. In the case when the dispersion curves for magnons and phonons intersect, which is observed for $v_{ph} < v_m$ at $\omega_0/J < 2$ (v_{ph} and v_m are the velocities of phonons and magnons, respectively), additional singularities are formed in the density of states of these quasiparticles. The calculations were made for ω_0/J = 1, 2, 4, 6, 8, and 10; the figures illustrate the typical cases when $\omega_0/J = 1$ and $\omega_0/J = 6$. Under the action of the magnetic system, the structural factor of lattice fluctuations shown in Fig. 1 becomes spatially anisotropic. Ladder-type fluctuations containing two nearest chains in the [01] direction and quasi-one-dimensional chain fluctuations in the [10] direction, which are separated by distance $r \approx 7$–10, are formed in the magnetic subsystem. The energy per bond in an antiferromagnet with a square lattice is 1.3 times smaller than the energy in an antiferromagnetic chain. Consequently, lattice fluctuations facilitate local extension of the lattice along one of the symmetry directions of the initial square lattice. Ladder-type fluctuations accompanied by dynamic local lattice dimerization also lower the magnetic energy; the approximated dependence of this energy has the form

$$|E_m(\alpha) - E_m(0)| \approx A(\alpha/\alpha_{c3})^{1.80(6)},$$

$$A = \begin{cases} 0.11(1), & v_m > v_{ph}, \\ 0.18(2), & v_m < v_{ph}. \end{cases}$$

The gain in the magnetic energy is almost an order of magnitude higher than the loss in the elastic energy.

The average displacement

$$U^{\beta}_{av} = \frac{1}{N}\sum_{i,j} u^{\beta}_{i,j}, \quad \beta = x([10]), y([01])$$

is depicted in Fig. 2. Anisotropy of lattice fluctuations leads to anisotropy of displacement $U^{x}_{av} - U^{y}_{av}$ (Fig. 2c) and lowers the crystal symmetry from tetragonal to orthorhombic. With increasing interaction between the magnetic and elastic subsystems, zero-point vibrations at a certain wave vector Q are enhanced, as well as their correlation $\langle U_i^2 U_j^2\rangle \propto \langle N(0)N(Q)\rangle$, depicted in Fig. 3. The maximal value of the correlator is attained at the wave vector $Q_{\max} = (0.75\text{–}0.9)\pi$, $\alpha_{c2} < \alpha < \alpha_{c3}$ and reflects a coherent vibration of ions with localized spin excitations in the [10] direction. For $v_m > v_{ph}$, in the interval $\alpha_{c2} < \alpha < \alpha_{c3}$ of the parameters, the local orthorhombicity parameter shown in Fig. 2c decreases sharply, its value being within the computational error. The change in the symmetry of structural distortions is in qualitative agreement with the replacement of the condensed mode $(\pi, 0)$ for $\delta < 0.5$ ($\delta = J_{i,i+1} - J_{i,i-1}$) by the optical mode (π, π) for $\delta > 0.5$, calculated on a square lattice by the method of exact diagonalization in the adiabatic approximation [13].

A qualitatively different behavior of elastic and magnetic properties is observed in the case when $v_m < v_{ph}$. The lattice volume and the orthorhombicity parameter increase monotonically for $\alpha > \alpha_{c2}$ and the change in zero-point vibrations is an order of magnitude smaller as compared to the case when $v_m > v_{ph}$ (Fig. 3a). Anisotropy of correlated vibrations also increases and the results of calculations can be correctly described by the power dependence

$$\langle U_\beta^2\rangle - \langle U_\gamma^2\rangle \approx 0.24(3)[(\alpha - \alpha_{c2})/\alpha_{c3}]^{0.41(3)}.$$

The changes in the lattice parameters in the region of the critical values $\alpha_{c2,3}$, in which the typical values of the upper boundary of the region of acoustic vibrations in quasi-two-dimensional antiferromagnets R_2CuO_4 (R = La, Gd, Eu, Nd) are $M \approx 4 \times 10^{-22} g$, and $\omega_0 = J$, are equal to

$$U_{c2} = 0.005(1)\ \text{Å}, \quad U_{c3} = 0.04(02)\ \text{Å}$$

for $\omega_0 \approx 4 \times 10^{12}$ Hz [14] and

$$U_{c2} = 0.002(1)\ \text{Å}, \quad U_{c3} = 0.007(2)\ \text{Å}$$

for $\omega_0 \approx 10^{14}$ Hz. The lattice-averaged change in the exchange interaction in the region of the antiferromagnet–quantum spin liquid phase transition constitutes approximately 1% ($dJ/J \approx 0.01$), which is an order of magnitude smaller than local exchange fluctuations.

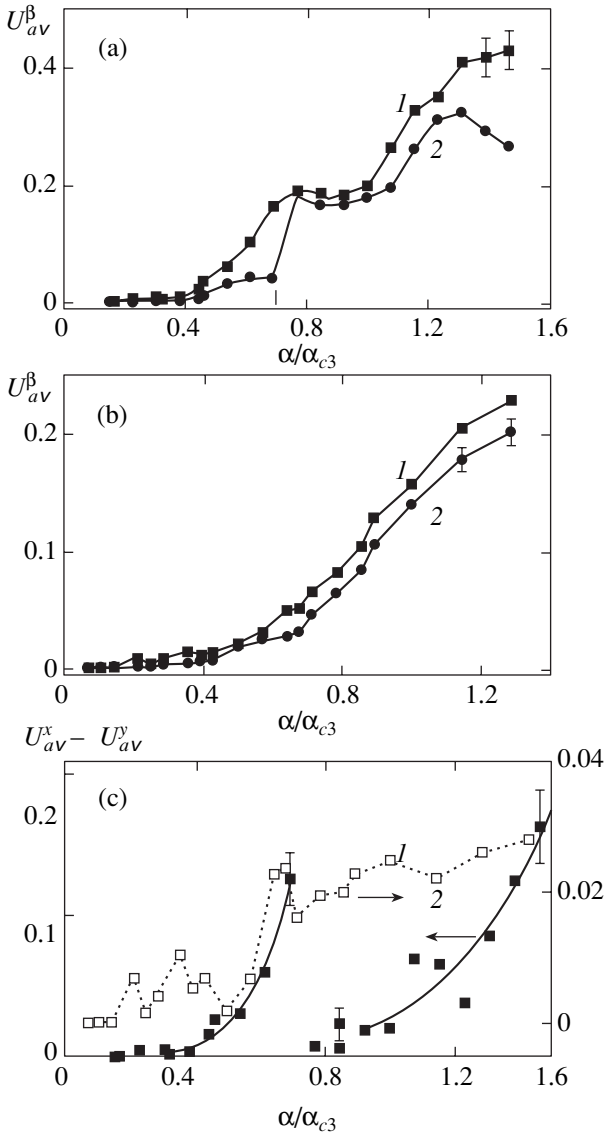

Fig. 2. Dependence of lattice-averaged displacements U^{β} of ions, normalized to $\sqrt{\hbar/M\omega_0}$, for $\omega_0/J = 1$ (a) and 6 (b) in directions $\beta = [10]$ (*1*) and [01] (*2*) on the normalized spin–phonon interaction constant and the dependence of the orthorhombicity parameter $U^{x}_{av} - U^{y}_{av}$ for $\omega_0/J = 1$ (*1*), 6 (*2*) on α/α_{c3} (c).

The linear decrease in the magnetic moment at a site upon an increase in the spin–phonon coupling constant can be approximated by the dependence

$$\frac{\sigma}{\sigma(0)} = \begin{cases} 1.14 - 1.3\alpha/\alpha_{c3}, & v_m > v_{ph}, \\ 1.12 - 0.96\alpha/\alpha_{c3}, & v_m > v_{ph}. \end{cases}$$

In the range of parameters $0.15 < \alpha/\alpha_{c3} < 0.7$. For $\alpha =$

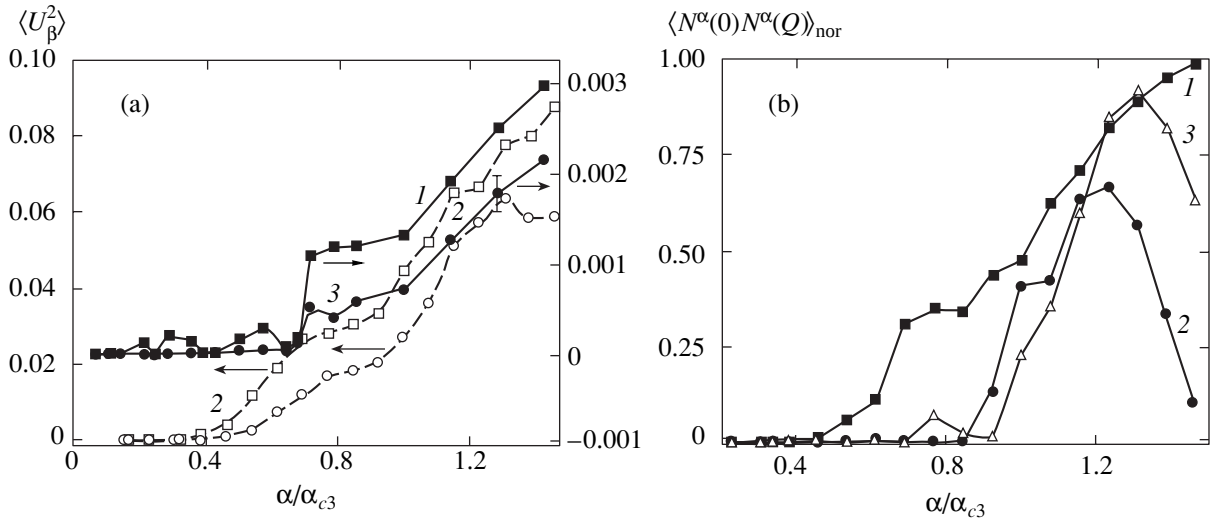

Fig. 3. Dependences (a) of the mean square displacement $\langle U_\beta^2 \rangle$ of ions normalized to $\hbar/M\omega_0$ for β = [10] (*1*, *2*) and [01] (*3*, *4*), $\omega_0/J = 1$ (*2*, *4*) and 6 (*1*, *3*) on the normalized spin–phonon interaction constant and (b) of the maximum value of the phonon density correlator on the wave vector Q for $\omega_0/J = 1$, β = [10] (*1*), [01] (*2*), and [11] (*3*) on α/α_{c3}.

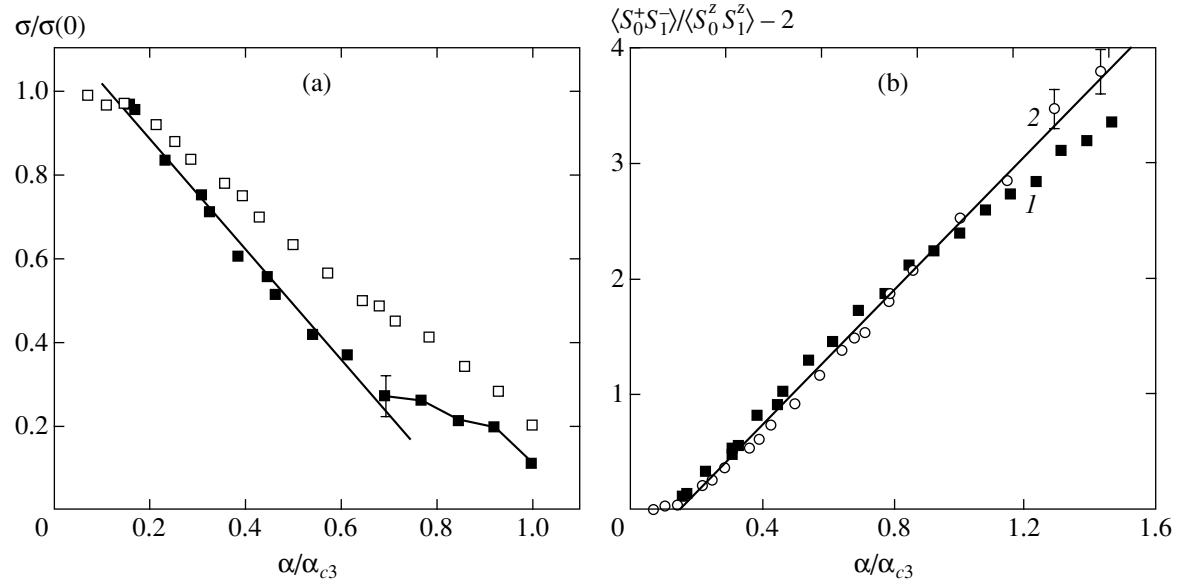

Fig. 4. Normalized magnetic moment $\sigma/\sigma(0)$ at a site (a) and the ratio of the correlation functions between the transverse components of spins and longitudinal components for $r = 1$ (b) for $\omega_0/J = 1$ (*1*) and 6 (*2*) as functions of the spin–phonon interaction parameter.

α_{c3}, the magnetic moment abruptly vanishes. The typical dependences are shown in Fig. 4a. In the region of the critical parameters of the spin–phonon coupling, the spin–spin correlation functions and the correlation radius are spatially anisotropic,

$$\left| 1 - \frac{\sum_r \langle S^z(i, j)S^z(i, j + r)\rangle}{\sum_r \langle S^z(i, j)S^z(i + r, j)\rangle} \right| \approx 0.02\text{–}0.04,$$

and anisotropy of the spin correlation functions between directions [11] and [10] is on the order of 0.1. For $\alpha > \alpha_{c1}$, the spherical symmetry of spin–spin correlation functions depicted in Fig. 4b is violated. This fact serves as a criterion for determining the value of the spin–phonon interaction parameter α_{c1} and is in qualitative agreement with the results obtained by Andreev and Grishchuk [8], who obtained a spin-nematic state in the Heisenberg model with competing antiferromagnetic interactions and the four-spin exchange. In the vicinity of the wave vector $Q = (\pi, \pi)$ corresponding to

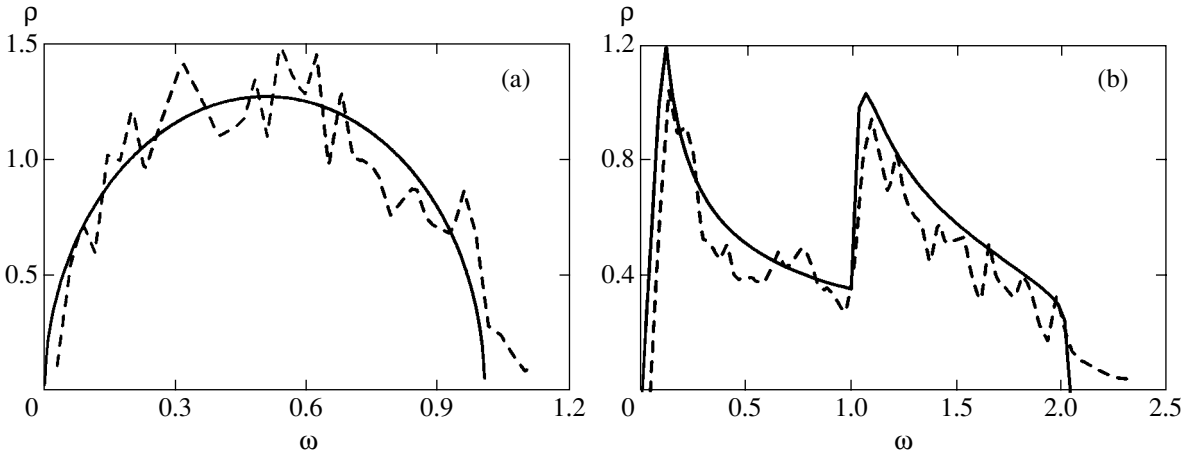

Fig. 5. Model densities of states defined analytically, $\rho(\omega) = (8/\pi)\sqrt{\omega(1-\omega)}$ (a) and numerically (b) (solid curves). The reconstructed density of states are depicted by the dashed curves.

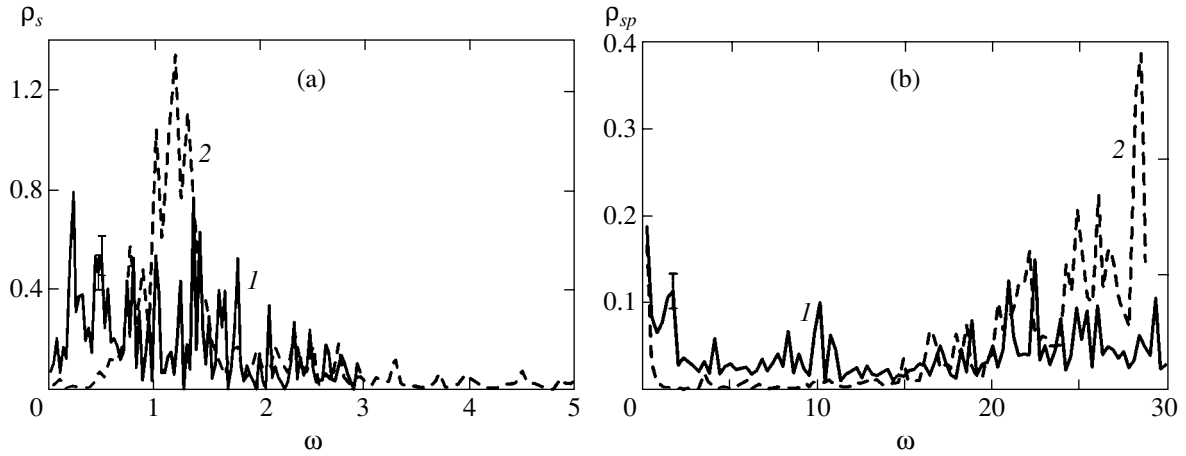

Fig. 6. Density of states for (a) spin and (b) coupled spin–phonon excitations for $\omega_0/J = 6$, $\alpha/\alpha_{c3} = 0.8$ (*1*) and 1.14 (*2*).

the antiferromagnetic structural factor, satellites with the incommensurability vector of the spin density are observed in the interval $q_{in} = (0.7–0.95)\pi$. The intensity of the satellites varies in the limits

$$\frac{S^z(q_{in})}{S^z(\pi,\pi)} \approx \begin{cases} 0.05, & \alpha = \alpha_{c1}, \\ 0.15, & \alpha = \alpha_{c2}, \\ 0.3, & \alpha = \alpha_{c3}. \end{cases}$$

The procedure of reconstructing the spectral density of states [12] for given models can be successfully used for determining the band boundaries and the positions of the peaks of the function $\rho(\omega)$ on the energy scale to within 5%. The intensity has a saw-tooth shape and fluctuates in the limits of 10–20%. Figure 5 shows the reconstructed and model densities of states defined analytically ($\rho(\omega) = (8/\pi)\sqrt{\omega(1-\omega)}$) and numerically. The time correlator

$$G(\tau) = \int_0^{\omega_{\max}} e^{-\omega\tau}\rho(\omega)d\omega$$

was calculated over 100 points τ_i, $i = 1, 2, \ldots, 100$. The typical densities of spin excitations and coupled spin–phonon excitations are shown in Fig. 6. For $\alpha > \alpha_{c2}$, a gap is observed in the spectral density of spin excitations. The dependence of the gap energy on the magnitude of the spin–phonon coupling, together with the approximating power function

$$\Delta_s/J \approx [(\alpha - \alpha_{c2})/\alpha_{c3}]^{0.50(8)}, \quad \omega_0 = J,$$

is depicted in Fig. 7 (solid curve). In the density of coupled spin–phonon excitations, one can single out a quasigap. The maximal density $\rho(\omega)$ corresponds to quasiparticles with zero energy and with the quasiparticle

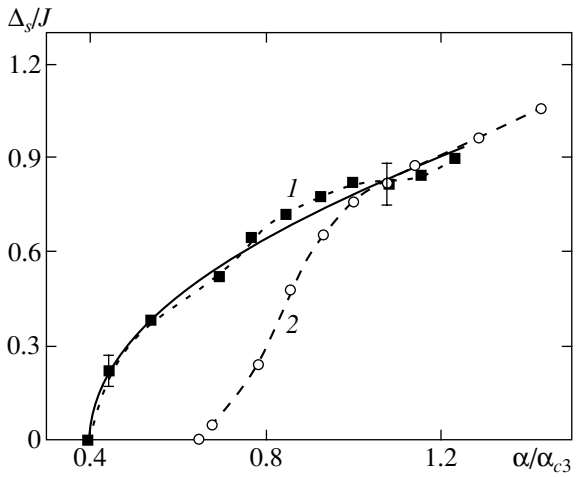

Fig. 7. The energy Δ_s of the gap in the spin excitation spectrum as a function of the spin–phonon interaction parameter for $\omega_0/J = 1$ (*1*) and 6 (*2*).

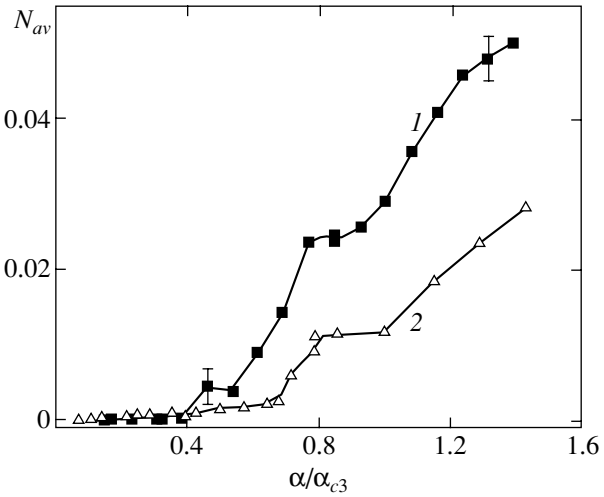

Fig. 8. Average occupation number for phonons as a function of the normalized spin–phonon interaction constant for $\omega_0/J = 1$ (*1*) and 6 (*2*).

excitation energy $\omega \approx 2(\omega_0 + 2J)$, $2(\omega_0 + J)$, and $3(\omega_0 + J)$ for $v_{ph} > v_m$ and $\omega \approx 4(\omega_0 + J)$ and $8(\omega_0 + J)$ for $v_{ph} < v_m$. For $\omega_0 \approx 4 \times 10^{12}$ Hz [14] and $J \approx 0.1$ eV, these estimates are in satisfactory agreement with the optical data on the absorption spectra of $Sr_2CuCl_2O_2$ [1], which show a broad peak in the vicinity of 4000 cm^{-1}, as well as with the values of excitation energy $E^{MC} \approx$ 4400 cm^{-1} calculated by the Monte Carlo method. The observed excitations reveal a close relation between the spin and lattice degrees of freedom in the CuO_2 plane.

On the plane including the upper boundary ω_0 of the region of acoustic vibrations and the spin–phonon coupling parameter α, three critical lines can be singled out. As the spin–phonon coupling constant attains the critical value with the approximation dependence $\alpha_{c1} = 0.16(2)\omega_0/J$, coupled spin–phonon excitations are formed analogously to the formation of polarons in systems with electron–phonon coupling. As the value of α increases, the quasiparticle density becomes higher and the spectral density $\rho(\omega = 0)$ of bound spin–phonon excitations has a finite value at $\omega = 0$ for $\alpha_{c2} = 0.39(6)(\omega_0/J)^{0.85(4)}$. A gap Δ_s appears in the spin excitation spectrum and the crystal symmetry is lowered. If we treat the gap width Δ_s as an order parameter of singlet pairs of spins, an inhomogeneous state consisting of a long-range magnetic order and a singlet state is realized in the range of parameters $\alpha_{c2} < \alpha < \alpha_{c3}$. This resembles the coexistence of the normal and anomalous phases in liquid helium and in a type II superconductor in a magnetic field. For constant α_{c3}, which can be approximated by the power dependence $\alpha_{c3} = 0.62(4)(\omega_0/J)^{0.85(6)}$, the long-range magnetic order disappears and a quantum spin liquid is formed.

The correlated state of lattice fluctuations can be destroyed by thermal phonons. The critical temperature can be estimated from the condition of equality of the thermal energy E_{heat} of phonons and the energy $E_{\text{bin}} = (N_{ph} - N_{ph,\,c2})\omega_0/2$ of the bound state of phonons. In the Debye approximation, $E_{\text{heat}} = 3\pi^4 k_B T^4/(5\Theta^3)$, where Θ is the Debye temperature, the corresponding critical temperature is

$$T^* \approx 0.74\Theta^{3/4}[0.02(\alpha - \alpha_{c3})/\alpha_{c3}]^{1/4}.$$

The dependence of the average number $N_{av} = (1/N)\sum_k N_k$ of phonons on the normalized value of the spin–phonon coupling constant is shown in Fig. 8. Lattice fluctuations are connected with magnetic fluctuations which change under the action of the magnetic field and temperature at $T \sim \Delta_s$. For $\alpha > \alpha_{c3}$, the lowest temperature at which the soliton lattice can be broken is determined by thermal phonons; for $\theta = 400$ K, we have $T^*_{c3} \approx 22$ K.

The low values of the magnetic moment $\sigma = 0.4(1)$ for Gd_2CuO_4 and Eu_2CuO_4 [15], which were obtained from elastic scattering of neutrons, as well as the values $\sigma = 0.35(4)$ determined from the electron spin resonances at Gd^{3+} ions in Eu_2CuO_4 [16], are probably due to the spin–phonon interaction with parameters $\alpha/\alpha_{c3} \approx$ 0.3 and 0.35 leading to the formation of coupled spin–phonon excitations. This changes the acoustic excitation spectrum. For example, an anomaly is observed in the lower branch of the acoustic phonon excitation spectrum along the ΓX direction in the isostructural compound Nd_2CuO_4 [14]. The corresponding changes in the lattice constant are on the order of 2×10^{-3} Å and are manifested in the X-ray spectra in the form of an ellipsoidal displacement of oxygen ions in the *ab* plane at right angles to the Cu–O bond [17].

The lifetime of coupled spin–phonon quasiparticles and the average relaxation time are proportional to the matrix element of the spin–phonon interaction operator for a phonon transition from the ground state to an excited state with a simultaneous change in the spin configurations of the two spins. In accordance with the "golden Fermi rule,"

$$\frac{1}{\tau_0} = \frac{2\pi}{\hbar}|\langle \text{exc}|\hat{V}_{sph}|0\rangle|^2 N_{ph},$$

the quasiparticle lifetime $\tau_0 = 0.6 \times 10^{-7}$ s ($\langle$exc| denotes the excited state). The relaxation time distribution is described by the power law $P(\tau) \propto (\tau/\tau_0)^{5/4}$ for $\tau < \tau_0$.

4. CONCLUSIONS

Let us summarize the main results. The interaction between the elastic and magnetic subsystems leads to anisotropy of the elastic vibrations of the lattice as well as in magnetic properties; the change in the latter properties occurs at the three characteristic parameters of the spin–phonon interaction. For $\alpha = \alpha_{c1}$, coupled lattice and spin fluctuations are formed and the spherical symmetry of the spin–spin correlation functions is broken. For $\alpha = \alpha_{c2}$, a gap opens in the spin excitation spectrum and the crystal symmetry is lowered. The singlet state and the long-range antiferromagnetic order may coexist. For $\alpha = \alpha_{c3}$, the magnetic moment at a site vanishes and the antiferromagnet–quantum spin liquid phase transition takes place. The constant of the spin–phonon coupling corresponding to a decrease in the magnetic moments of quasi-two-dimensional antiferromagnets Gd_2CuO_4 and Eu_2CuO_4 are determined.

REFERENCES

1. V. V. Struzhkin, A. F. Goncharov, H. K. Mao, *et al.*, Phys. Rev. B **62**, 3895 (2000).
2. N. Ichikawa, S. Uchida, J. M. Tranquada, *et al.*, Phys. Rev. Lett. **85**, 1738 (2000).
3. T. Dahm, Phys. Rev. B **61**, 6381 (2000).
4. J. Takeya, Y. Ando, S. Komiya, *et al.*, Phys. Rev. Lett. **88**, 077001 (2002).
5. E. I. Golovenchits, V. A. Sanina, A. A. Levin, *et al.*, Fiz. Tverd. Tela (St. Petersburg) **39**, 1600 (1997) [Phys. Solid State **39**, 1425 (1997)].
6. V. A. Pashchenko, S. Huant, A. A. Stepanov, and P. Wyder, Phys. Rev. B **61**, 6889 (2000).
7. A. A. Stepanov, P. Wyder, T. Chattopadhyay, *et al.*, Phys. Rev. B **48**, 12979 (1993).
8. A. F. Andreev and I. A. Grishchuk, Zh. Éksp. Teor. Fiz. **87**, 467 (1984) [Sov. Phys. JETP **60**, 267 (1984)].
9. S. S. Aplesnin, Fiz. Tverd. Tela (St. Petersburg) **39**, 1404 (1997) [Phys. Solid State **39**, 1246 (1997)].
10. N. V. Prokof'ev and B. V. Svistunov, Phys. Rev. Lett. **81**, 2514 (1998); N. V. Prokof'ev, B. V. Svistunov, and I. S. Tupitsyn, Zh. Éksp. Teor. Fiz. **114**, 570 (1998) [JETP **87**, 310 (1998)].
11. M. Suzuki, J. Stat. Phys. **43**, 883 (1986).
12. A. S. Mishchenko, N. V. Prokof'ev, A. Sakamoto, and B. V. Svistunov, Phys. Rev. B **62**, 6317 (2000).
13. S. Tang and J. E. Hirsch, Phys. Rev. B **37**, 9546 (1988).
14. E. Rampf, U. Schröder, F. W. de Wette, *et al.*, Phys. Rev. B **48**, 10143 (1993).
15. T. Chattopadhyay, J. W. Lynn, N. Rosov, *et al.*, Phys. Rev. B **49**, 9944 (1994).
16. C. Rettori, S. B. Oseroff, D. Rao, *et al.*, Phys. Rev. B **54**, 1123 (1996).
17. P. Adelman, R. Ahrens, G. Czjzek, *et al.*, Phys. Rev. B **46**, 3619 (1992).

Translated by N. Wadhwa